

## Elaboration and Characterization of Sprayed Tb-Doped ZnO Thin Films

<sup>1</sup> Amina ELFAKIR, <sup>1</sup> Abdeslam DOUAYAR, <sup>2</sup> Raquel DIAZ,  
<sup>1</sup> Imane CHAKI, <sup>2</sup> Pilar PRIETO, <sup>1</sup> Mohamed LOGHMARTI,  
<sup>1</sup> Azzam BELAYACHI and <sup>1</sup> Mohammed ABD-LEFDIL

<sup>1</sup> Université Mohammed V-Agdal, Faculté des Sciences, LPM, B.P. 1014, Rabat, Morocco

<sup>2</sup> Departamento de Física Aplicada, Universidad Autónoma de Madrid, Spain

<sup>1</sup> Tel./ fax: +212 (0) 537778973,

E-mail: a-lefdil@fsr.ac.ma

Received: 31 December 2012 / Accepted: 10 August 2013 / Published: 26 May 2014

**Abstract:** ZnO and Tb-doped ZnO (TZO) thin films were deposited on glass substrate at 350 °C by spray pyrolysis technique. Structural, optical and electrical properties of the films were investigated as a function of dopant concentration, which was varied between 0 and 5 at % of terbium. TZO films were polycrystalline and exhibit hexagonal quartzite crystal structure with a preferential orientation along [002] direction. The AFM measurements show that the roughness of the films increased with Tb doping. All the TZO films exhibit a transmittance between 70 and 80 % in the visible range. The TZO films were n-type degenerate semiconductor with a lowest electrical resistivity of about  $6.0 \times 10^{-2} \Omega \cdot \text{cm}$ . Copyright © 2014 IFSA Publishing, S. L.

**Keywords:** Spray pyrolysis, Thin films, Tb-Doped ZnO, Characterization.

### 1. Introduction

Zinc oxide has emerged as one of the most promising oxide materials due to its high chemical stability, wide direct band gap of 3.3 eV and large exciton binding energy of about 60 meV at room temperature [1]. It is attractive in many technological fields such as solar cells [2] and gas sensors [3, 4]. To improve the physical properties of ZnO films, various elements (from group III, group IV and rare earths) have been used [5-10]. Tb doped ZnO thin films have been deposited by several techniques like sputtering [11, 12] and sol-gel [13].

In this paper, we have focused our attention to investigate the effect of Tb doping on structural, optical and electrical properties of TZO thin films. Among all the preparation techniques mentioned

above, we have used chemical spray pyrolysis technique because it is simple, low cost and can be used for the large area depositions.

### 2. Experimental

The samples of  $\text{Zn}_{1-x}\text{Tb}_x\text{O}$  thin films were deposited on glass substrates by spray pyrolysis technique. The starting solution consisted of zinc chloride ( $\text{ZnCl}_2$ ) at a concentration of 0.05 M, dissolved in distilled water, where the water volume contained per liter of solution was fixed to 200 ml. The doping was achieved by the addition of terbium (III) chloride ( $\text{TbCl}_3$ ) to the solution, with a molar concentration of 0.05 M. The [Tb]/ [Zn] atomic percent ratio explored in the solution were 0, 1, 3 and

5 at %. The substrate temperature was fixed to 350 °C and the solution was sprayed at a flow rate of 2.6 ml/min. X'Pert Pro diffractometer was used to determine the X-Ray Diffraction (XRD) patterns with Cu K $\alpha_1$  radiation ( $\lambda = 1.54056\text{\AA}$ ). The optical transmittance of Tb-ZnO thin films was investigated by an UV/VIS spectrophotometer (Cary 17D). Photoluminescence (PL) measurements were performed at room temperature in the visible range using a 355 nm line of a frequency-tripled neodymium-doped yttrium aluminum garnet-Nd-YAG-laser. Mobility, resistivity and carrier concentration were determined at room temperature with an ECOPIA Hall effect measurement system.

### 3. Results and Discussion

#### 3.1. Structural Properties

Fig. 1 shows the spectra of TZO thin films for different [Tb]/ [Zn] contents. From the X-ray diffraction spectra, it can be seen that all the films are polycrystalline and the position of the peaks fit well to ZnO wurtzite structure. Under the resolution limit for this analytical technique, no extra phases involving terbium compounds were detected, even for the highest percentage of Tb doping.

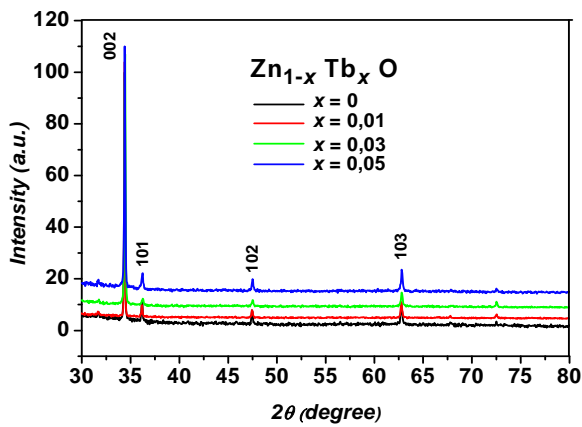


Fig. 1. XRD patterns of Zn<sub>1-x</sub>Tb<sub>x</sub>O thin films.

A preferential orientation along [002] direction was always obtained and some weak orientations such as (101), (102) and (103) have also been observed but with small intensities.

Quantitative information concerning the preferential crystallite orientation is obtained from the texture coefficient TCs (hkl) defined by this relation [14]:

$$TC(hkl) = \frac{I(hkl)/I_o(hkl)}{N^{-1} \sum_N I(hkl)/I_o(hkl)}, \quad (1)$$

where  $I(hkl)$  is the measured relative intensity of a plane (hkl),  $I_o(hkl)$  is the standard intensity of the plane (hkl) taken from JCPDS data [89-1397],  $N$  is the number of diffraction peaks. It can be seen that TC (002) decreases slightly and continuously with Tb doping indicating a weak reorientational effects with increasing Tb content. The values of lattice parameters  $c$  and  $a$  were found around 0.5210 nm and 0.3190 nm respectively, which is in agreement with the usually published values for ZnO. The crystallite size  $D$  was calculated using Scherrer's formula [15] and the values were in 95 nm-70 nm.

$$D = \frac{0.9\lambda}{B \cos \theta}, \quad (2)$$

#### 3.2. Morphological Properties

The surface morphology of the undoped and Tb doped ZnO thin films, deposited on glass substrates and analyzed by atomic force microscopy (AFM), are shown in Fig. 2. The root mean square (rms) of the samples was calculated from AFM images and the obtained values are presented in Table. 1.

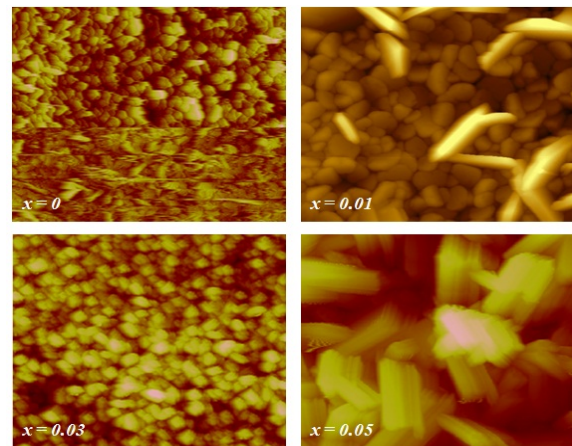


Fig. 2. AFM images of Zn<sub>1-x</sub>Tb<sub>x</sub>O thin films.

One can note that the surface morphology of the films is influenced by the terbium doping since the roughness of the surface increases sharply with terbium doping content higher than 1 % which may be the result of the accumulation of the Tb on interstitial sites of ZnO matrix.

Table. 1. Structural parameters of Zn<sub>1-x</sub>Tb<sub>x</sub>O thin films.

x (at.%)	RMS (nm)	TC (002)
0	30	3.0
0.01	36	2.9
0.03	77	2.7
0.05	108	2.3

### 3.3. Optical Properties

Fig. 3 displays the total transmittance (specular + diffusion) and specular reflectance spectra of the undoped and TZO thin films, measured in the wavelength range from 300-2200 nm at room temperature. It can be observed that all the TZO thin films exhibit high transparency in both visible and near infrared region. The absence of contrasted fringes in the transmission spectra is related to the diffusion phenomenon in agreement with the small grain size, as determined by XRD measurements. The low measured specular reflectance reflects the predominance of the diffusion component of the total reflectance, in agreement with the high values of rms reported below.

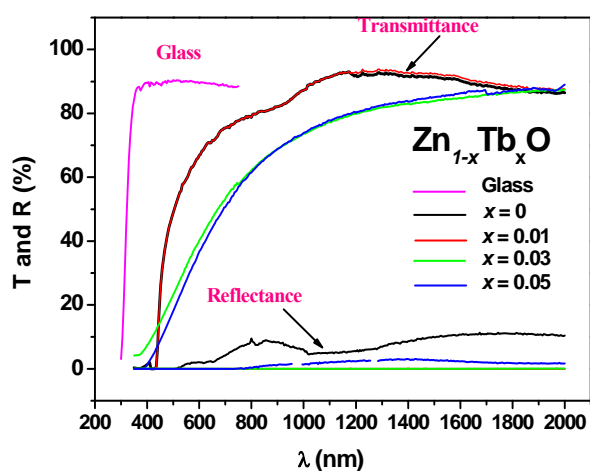


Fig. 3. Transmittance and reflectance UV – NIR spectra of  $Zn_{1-x}Tb_xO$  thin films.

### 3.4. Photoluminescence Properties of Films

Photoluminescence (PL) spectra of TZO thin films performed at room temperature are illustrated in Fig. 4.

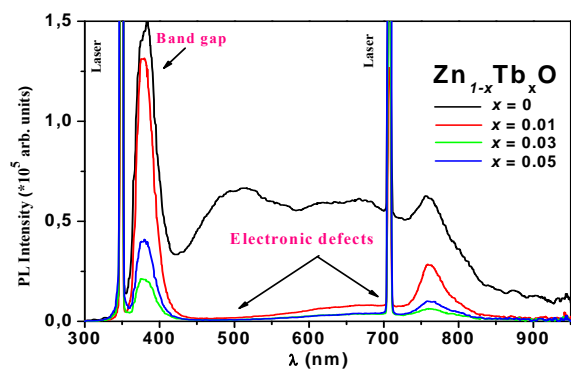


Fig. 4. PL spectra of the  $Zn_{1-x}Tb_xO$  thin films.

From the PL spectra, we note the occurrence of two peaks of the laser line, the first at 355 nm and the

second at 705 nm. All the films exhibit excitonic peak centered at 379 nm attributed to the radiative recombination of electron-hole pairs.

The second order of this PL band is visible at 760 nm. The wide PL band centered at 510 and 697 nm characteristic of deep levels of oxygen vacancies in the ZnO matrix, and zinc or oxygen atoms in interstitial position, as it was previously reported for ZnO thin films [16, 17].

The intensity of this wide band gap decreases with increasing Tb % content. No emission from  $Tb^{3+}$  ions is observed in the 400-1000 nm wavelength range indicating that there is no energy transfer from ZnO into  $Tb^{3+}$  ions in our samples.

### 3.5. Electrical Properties

The values of the Hall mobility  $\mu$ , the electrical resistivity  $\rho$  and the carrier density  $n$  of TZO thin films are summarized in Table 2. We note that the electrical parameters are dependent of the doping concentration. The electrical resistivity decreases from  $6.5 \times 10^{-1} \Omega \cdot \text{cm}$  for undoped ZnO to a value of  $6.0 \times 10^{-2} \Omega \cdot \text{cm}$  when the Tb content was increased to 1 at%. For larger Tb content, the resistivity increases which suggests that further doping do not leads to  $Tb^{3+}$  ions in substitution of the Zn ions, but to the appearance of new defects not necessarily optically active ( $Tb$  in interstitial positions). The solubility of  $Tb^{3+}$  ion is expected to be small and much lower than that of  $Yb^{3+}$ , in relation to the ionic radii difference between these elements ( $Tb^{3+}$ : 0.92 Å and  $Yb^{3+}$ : 0.87 Å [18]).

Table 2. Electrical parameters of  $Zn_{1-x}Tb_xO$  thin films at room temperature.

x (at. %)	$\rho$ ( $10^{-2} \Omega \cdot \text{cm}$ )	$\mu$ ( $10^{-1} \text{ cm}^2/\text{V.s}$ )	N ( $10^{19} \text{ cm}^{-3}$ )
0	65.0	7.3	1.30
0.01	6.0	8.4	12.5
0.03	7.4	10.3	8.20
0.05	7.7	7.7	10.6

## 4. Conclusions

$Zn_{1-x}Tb_xO$  thin films were prepared using the spray pyrolysis technique. The structure of the films is not sensitively modified by Tb incorporation while the surface morphology of the films is dependent on the Tb content. All the films show high transmittance in visible and near infrared regions. The intensity of PL wide band decreases with doping and no emission from  $Tb^{3+}$  ions is observed in the 400-1000 nm wavelength range indicating that there is no energy transfer from ZnO into  $Tb^{3+}$  ions in our samples. The lowest electrical resistivity was around  $6.0 \times 10^{-2} \Omega \cdot \text{cm}$  obtained for 1 % Tb content.

## Acknowledgements

We would like to thank Dr. Khalid Nouneh from MAScIR Rabat-Morocco for his help in AFM measurements.

## References

- [1]. S. J. Pearton, D. P. Norton, K. Ip, Y. W. Heo, and T. Steiner, Recent progress in processing and properties of ZnO, *Prog. Mater. Sci.*, Vol. 50, 2005, pp. 293-340.
- [2]. Changhyun Lee, Koengsu Lim, Jinsoo Song, Highly textured ZnO thin films doped with indium prepared by the pyrosol method, *Solar Energy Materials & Solar Cells*, Vol. 43, Issue 1, 1996, pp. 37-45.
- [3]. P. Rai, Y.-S. Kim, H.-M. Song, M.-K. Song, Y.-T. Yu, The role of gold catalyst on the sensing behavior of ZnO nanorods for CO and NO<sub>2</sub> gases, *Sensors and Actuators B: Chemical*, Vol. 165, Issue 1, 2012, pp. 133-142.
- [4]. Y. Zeng, L. Qiao, Y. Bing, M. Wen, B. Zou, W. Zheng, T. Zhang, G. Zou, Development of microstructure CO sensor based on hierarchically porous ZnO nanosheet thin films, *Sensors and Actuators B: Chemical*, Vol. 173, 2012, pp. 897-902.
- [5]. A. Douayar, R. Diaz, F. Cherkaoui El Moursli, G. Schmerber, A. Dinia, and M. Abd-Lefdil, Fluorine-doped ZnO thin films deposited by spray pyrolysis technique, *Eur. Phys. J. Appl. Phys.* Vol. 53, Issue 02, 2011, pp. 20501-p4.
- [6]. I. Soumahoro, G. Schmerber, A. Douayar, S. Colis, M. Abd-Lefdil, N. Hassanain, A. Berrada, D. Muller, A. Slaoui, H. Rinnert and A. Dinia, Structural, optical, and electrical properties of Yb-doped ZnO thin films prepared by spray pyrolysis method, *J. Appl. Phys.* Vol. 109, 2011, 33708.
- [7]. A. Douayar, A. Belayachi, M. Abd-Lefdil, K. Nouneh, Z. Laghfour, I. V. Kityk, A. Slezak, R. Miedzinski. Optical operation by electrooptical features of ZnO nanocrystalline films doped by Tm<sup>3+</sup> ions, *Journal of Alloys and Compounds*, Vol. 550, 2013, pp. 345-347.
- [8]. H. J. Ko, Y. F. Chen, S. K. Hong, H. Wenisch, T. Yao, D. C. Look, Ga-doped ZnO films grown on GaN templates by plasma-assisted molecular-beam epitaxy, *Applied Physics Letters*, Vol. 77, 2000, pp. 3761-3763.
- [9]. Ellmer Klaus, Klein Andreas, Rech Bernd (Eds.). Transparent conductive Zinc Oxide: Basics and Applications in Thin Film, *Springer Series in Materials Science*, New York, 104, 2008, p. 140.
- [10]. Y. Terai, K. Yamaoka, K. Yoshida, T. Tsuji, Y. Fujiwara, Photoluminescence properties of Eu-doped ZnO films grown by sputtering- assisted metalorganic chemical vapor deposition, *Physica E*, Vol. 42, 2010, pp. 2834-2836.
- [11]. Z. B. Fang, Y. S. Tan, H. X. Gong, C. M. Zhen, Z. W. He, Y. Y. Wang, Transparent conductive Tb-doped ZnO films prepared by rf reactive magnetron sputtering, *Materials Letters*, Vol. 59, 2005, pp. 2611-2614.
- [12]. Z. Wu, X. C. Liu, J. C. A. Huang, Room temperature ferromagnetism in Tb doped ZnO nanocrystalline films, *Journal of Magnetism and Magnetic Materials*, Vol. 324, 2012, pp. 642-644.
- [13]. Tiekun Jia, Weimin Wang, Fei Long, Zhengyi Fu, Hao Wang, Qingjie Zhang, Synthesis, characterization and luminescence properties of Y-doped and Tb-doped ZnO nanocrystals, *Materials Science and Engineering B*, Vol. 162, 2009, pp. 179-184.
- [14]. S. S. Shinde, P. S. Shinde, S. M. Pawar, A. V. Moholkar, C. H. Bhosale, and K. Y. Rajpure, Physical properties of transparent and conducting sprayed fluorine doped zinc oxide thin films, *Solide State Sci.* Vol. 10, Issue 9, 2008, pp. 1209-1214.
- [15]. P. Scherrer, *Gottinger Nachrichten*, Vol. 2, 1918, p. 98.
- [16]. J. Petersen, C. Brimont, M. Gallart, O. Crégut, G. Schmerber, P. Gilliot, B. Hönerlage, C. Ulhaq-Bouillet, J. L. Rehspringer, C. Leuvrey, S. Colis, A. Slaoui, and A. Dinia. Optical properties of ZnO thin films prepared by sol-gel process, *Microelectron. J.*, Vol. 40, 2009, pp. 239-241.
- [17]. Z. W. Liu, C. K. Ong, T. Yu, Z. X. Shen, Catalyst-free pulsed-laser-deposited ZnO nanorods and their room-temperature photoluminescence properties, *Applied Physics Letters*, Vol. 88, 2006, 053110.
- [18]. R. D. Shannon, *Acta Crystallographica Section A*, Vol. 32, 1976, pp. 751-926.